The Sodium LGS Brightness Model over the SOR

Jack Drummond, Steve Novotny, Craig Denman Paul Hillman, John Telle

Starfire Optical Range, Directed Energy Directorate, Air Force Research Laboratory
Kirtland AFB, New Mexico 87117-5776 USA

Mark Eickhoff

Boeing LTS, The Boeing Company, PO Box 5670, Kirtland AFB, NM 87185 USA

Robert Fugate

New Mexico Institute of Mining and Technology
801 Leroy Place, Socorro, New Mexico 87801 USA

ABSTRACT

A relatively simple formulation is developed for predicting the brightness of a sodium laser guidestar over the Starfire Optical Range (Longitude = 106° W, Latitude = +35 N) taking into account the power and polarization of our 50 W fasor (frequency-addition source of optical radiation), atmospheric extinction, distance to the mesosphere, time of year, and the Earth's magnetic field. The formulation is extended to Maui (Lon = 156° W, Lat = +21° N).

1. INTRODUCTION

During the course of sky testing two atomic sodium pump fasors (frequency-addition source of optical radiation [1-7]) that produce 20 and 50 W of power, respectively, we have developed a model for the brightness of a laser guidestar (LGS) over the Starfire Optical Range (SOR), a facility owned and operated by the Air Force Research Laboratory's Directed Energy Directorate on Kirtland Air Force Base near Albuquerque, New Mexico. The model is a distillation of five years of experiments [8-11] and involves many simplifying generalizations based on data fitting. This model can also be extended to the skies over Maui.

2. LASER GUIDESTAR BRIGHTNESS

The brightness of our LGS depends on five factors: 1) fasor power and polarization, 2) atmospheric extinction, 3) distance to the LGS in the mesosphere, 4) the sodium column density and 5) the Earth's magnetic field. Furthermore, by combining or overlapping the two fasors tuned to the D2a and D2b lines, respectively, it is possible to increase the brightness of the LGS to more than the simple sum of the two fasors. Eq 1 describes the dependence of the LGS brightness on fasor power

$$F = a \log(1 + w/w_0) \quad , \tag{1}$$

where F is the brightness of the return from the LGS at the top of the telescope in ph/s/cm^2, w is the power out of the fasor, and w_0 is a saturation power. Because of optical pumping, when the fasor is tuned to the D2a frequency with circular polarization, there is little saturation and an almost linear increase of brightness with power. However, there is much stronger saturation when the fasor is linearly polarized,

or when the D2b line is pumped with either circular or linear polarization. Figure 1 shows the results for the most recent power run for circular and linear polarization, where it is obvious that linear saturates more than circular polarization. Also shown in Fig 1 is the slope at the origin, $S = dF/dw = a/w_0$, which should be directly related to the sodium column density. From five years of testing, we find that S for linear polarization is generally 2/3 of the circular polarization S.

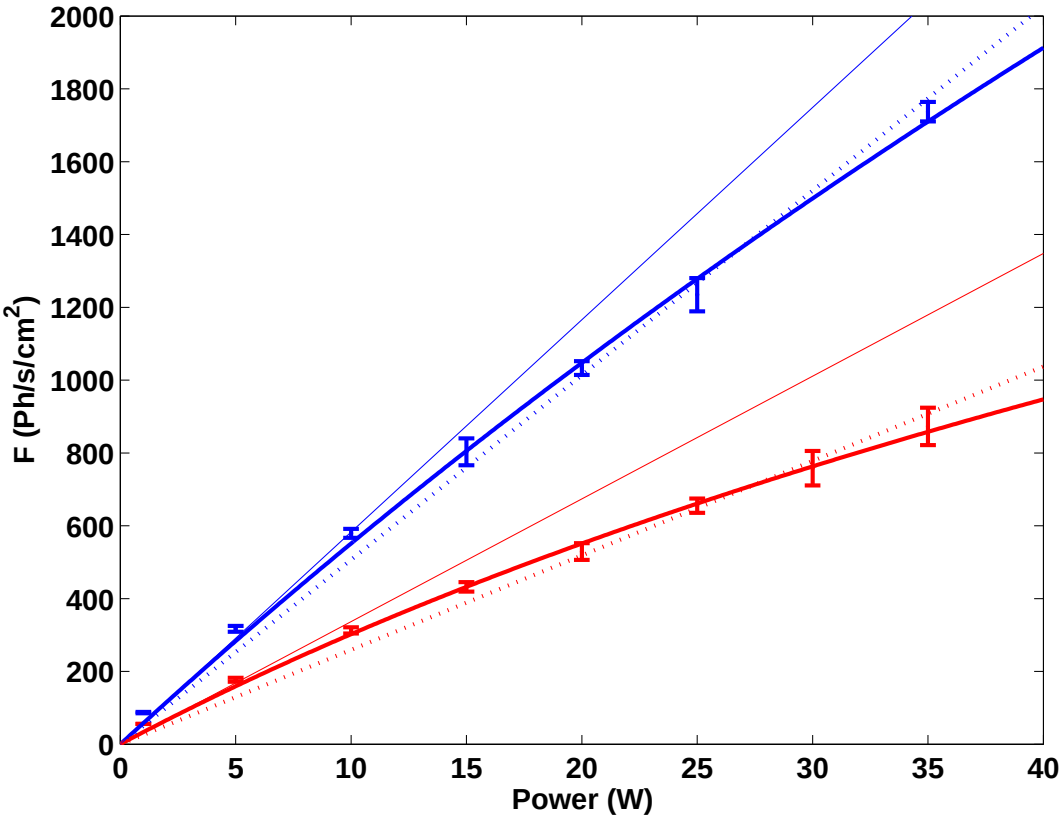

Figure 1. Power run on April 25, 2007 at the zenith. Circular polarization data is blue and linear is red. Dotted lines are simple linear fits and thinner lines are the slopes at the origin.

Because the brightness of the LGS falls off as $1/r^2$, but is proportional to the slant distance through sodium layer, which is in turn proportional to the distance r, to normalize the brightness of the LGS to zenith observations, F in Eq 1 should be increased by $r = X = 1/\sin el$, where X is the airmass and el is the elevation of the observation. To normalize observations at the zenith to the mesosphere, it is necessary to account for atmospheric transmission t for both the up and down legs by dividing F in Eq 1 by t and multiplying w and w_0 by t, which then means that S should be divided by t^2 to yield the slope at the origin in the mesosphere, S_0. Away from the zenith, to correct to the mesosphere, use t^X, rather than t, and t^{2X} rather than t^2.

3. SEASONAL VARIATION OF SODIUM COLUMN DENSITY

Plotting S_0 for all of our observations in Fig 2 reveals an annual variation of S_0 and presumably the sodium column density. The fits shown in Fig 2 are from

$$S_0 = A + B\cos((d - d_0)2\pi/365), \qquad 2$$

where d is the day number since January 0, d_0 is the day of maximum 320, $A = 158$ and $B = 109$ for circular polarization. For linear polarization A and B are 2/3 of the circular polarization values.

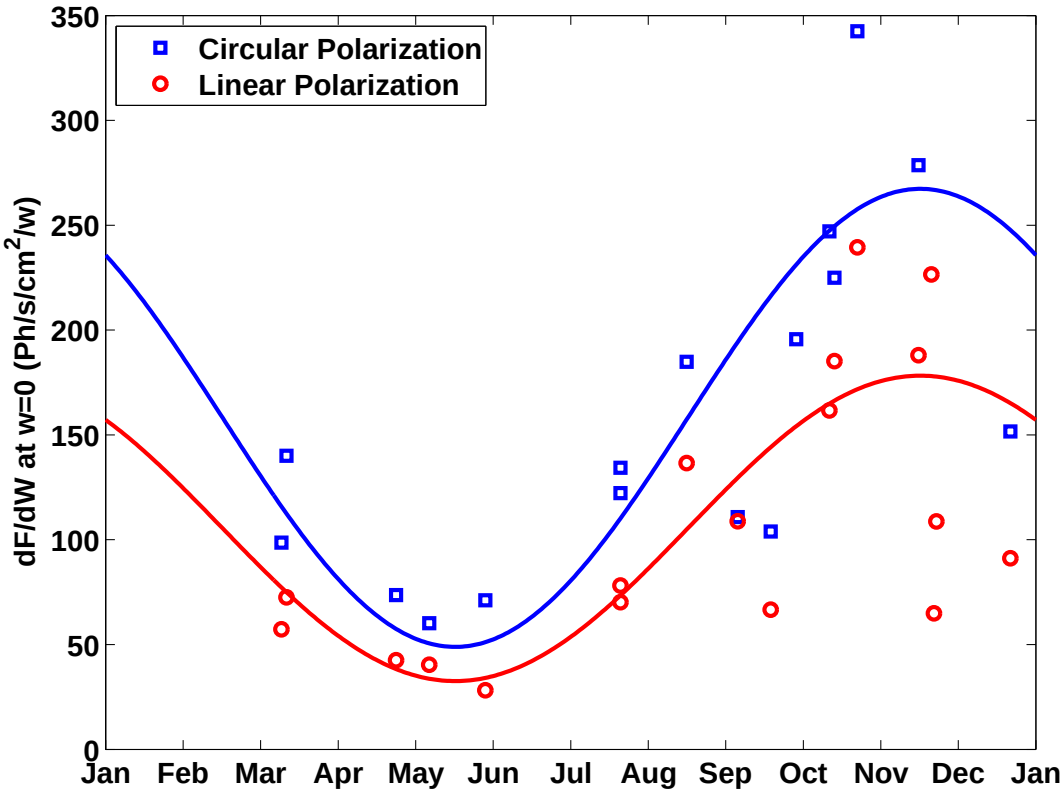

Figure 2. Annual S_0 (proportional to sodium column density) variation. The solid lines are from a simultaneous fit of the circular and linear polarization data with Eq 2, where the linear polarization S_L is always 2/3 of S_C. The largest residuals occur on November 16, during the night that the Earth goes through the Leonid meteor stream, and this may cause a spike over and beyond the annual cycle.

An alternate expression for Eq 1 where F has been corrected to the mesosphere at the zenith, is

$$F_0 = S_0 t^X w \, [1 - 0.236 \log(1 + t^X w/50.6655)] \quad . \qquad 3$$

Eq 3, together with the S_0 given by Eq 2, gives a formula for predicting the flux from the LGS in the mesosphere at zenith for any time of year.

4. NOCTURNAL SODIUM COLUMN DENSITY VARIATION

There has been some concern about the effect of the variation of the sodium column density during the night on the LGS brightness. Chet Gardner [12,13] has measured the sodium column density over both the SOR and Maui. Fig 4a from that paper for the SOR appears to show a strong variation in sodium column density during the night, with a minimum around 3:30 UT (20:30 MST) and maxima around 00:30 UT (17:30 MST) and 12:00 UT (5:00 MST), from the average of measurements made throughout the year. However, because of the way they weighted their observations, and because of correlations between the early and late hours of the night with seasonal mean densities, the figure is misleading. Since the average hourly densities were weighted by the number of lidar profiles, this gave far too much weight to November measurements when the sodium column densities are at their highest and when they took four

times more data in the early morning hours than at any other time of the year. Because the nights are longer in winter, when the mean column density is generally higher, the early and late hours are biased towards higher densities which leads to the impression of increasing densities near sunrise and sunset. For instance, the only contributions to the 01:00 UT (18:00 MST) hour comes from the three months of October, December and January, and to the 13:00 UT (6:00 MST) hour from November, December and January, with a few from March.

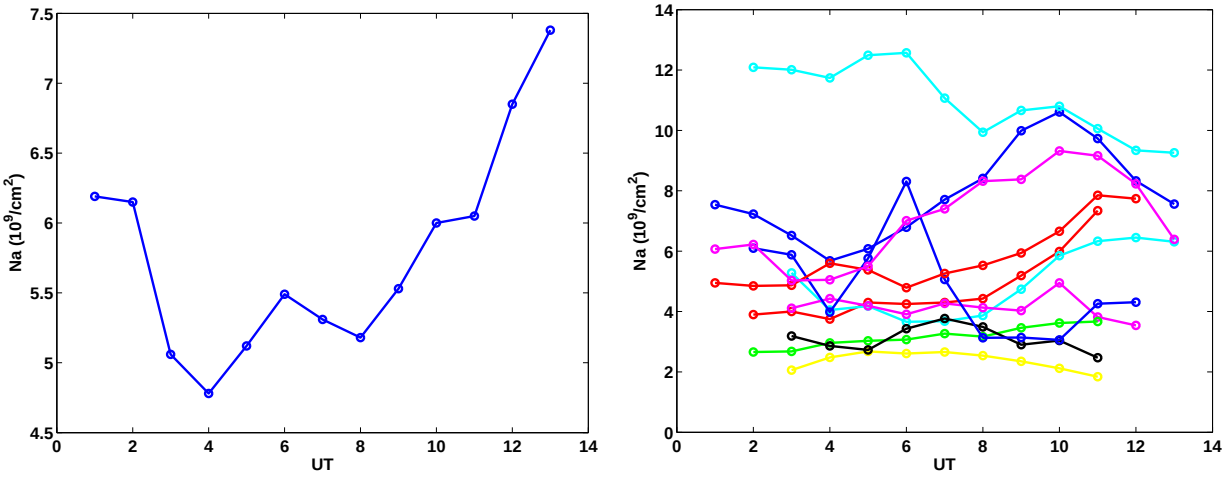

Figure 3. Nocturnal variation of sodium column density over the SOR from lidar data. The left plot shows the unweighted mean from through the year, while the right plot shows the measurements by month.

The left half of Fig 3 here shows their unweighted mean hourly density measurements. (The actual data used here were taken from tables in a preprint that were not in the published paper.) However, even this is misleading because the hourly variation is swamped by the variation in the mean throughout the year, as shown by the right half of Fig 3. In the end we conclude that the nocturnal variation of sodium column density is irregular, or at most, semi-regular. For planning purposes it is best to simply use the prediction from the seasonal variation, but cognizant that the density can vary by ±20% during the night.

5. IMPACT OF EARTH'S MAGNETIC FIELD

Another consideration is the impact of the Earth's magnetic field on the brightness of the LGS. We have previously reported [11] that the brightness variation of the LGS as the fasor is pointed at various elevations and azimuths could be fit with spherical coordinates that centered on the direction of the magnetic field lines. This is not quite right; it only depends on the sine of the angular distance δ between the fasor pointing and the direction of the field lines. When the fasor is pointing along the field lines at $az = 190°$ and $el = +62°$ (the apparent magnetic pole) for the SOR, the LGS is brightest because the magnetic field is not disrupting the optical pumping with circular polarization. Pumping with linear polarization is not affected by the magnetic field, and in fact, pumping with circular polarization 90° from the magnetic pole produces an LGS only as bright as pumping with linear polarization. The expression for the magnetic field brightness dependence factor for circular polarization is

$$f = 1.45 - 0.95 \sin \delta \qquad 4$$

which at the zenith is unity for the SOR and at $\delta = 90°$ is 0.5, equivalent to linear polarization, which is 0.5 everywhere.

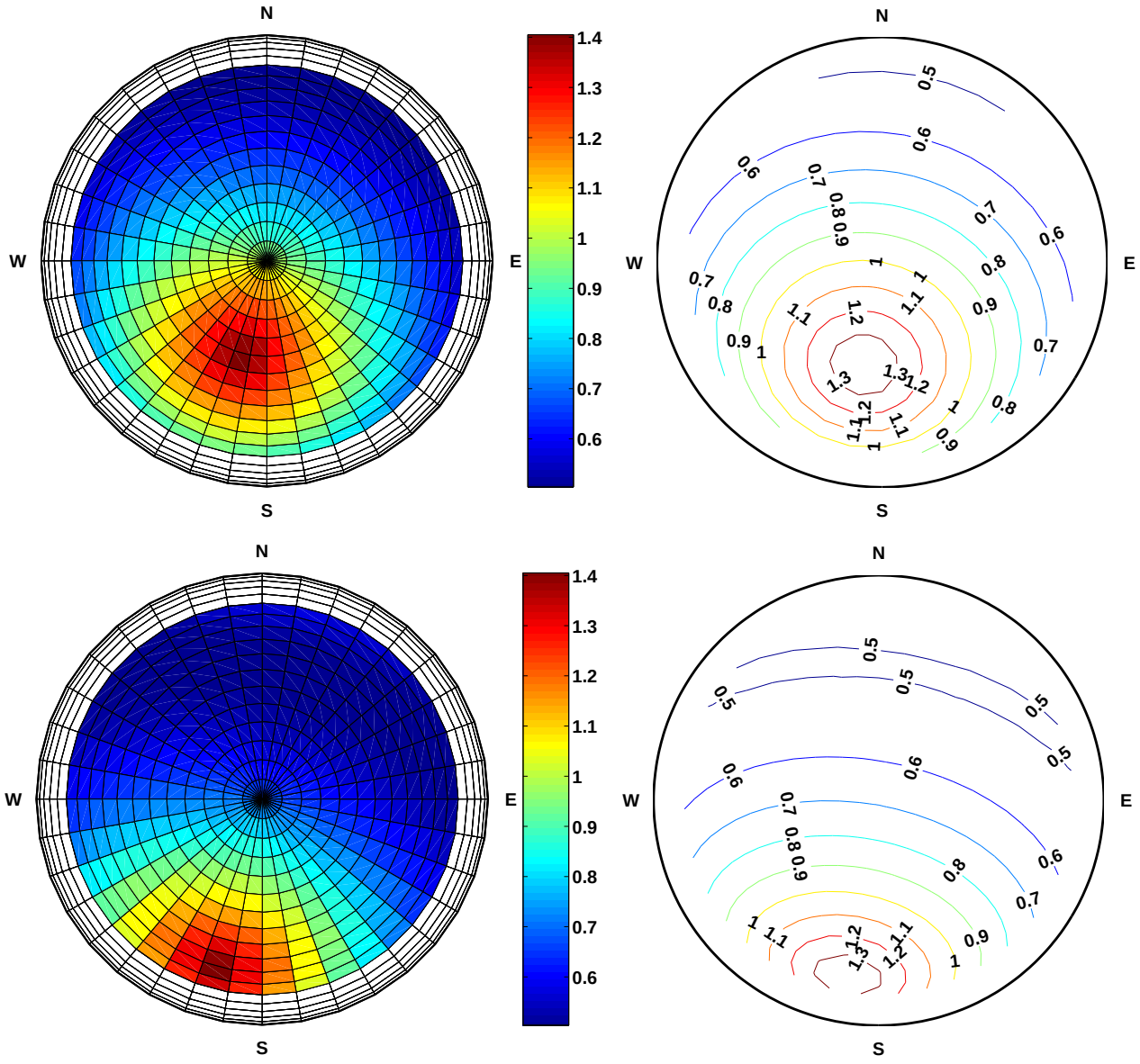

Figure 4. Surface and contour plots of the magnetic field factor (Eq 4) for the SOR (top) and Maui (bottom). The known direction where the magnetic field points to the SOR is the center of the contours at $az = 190°, el = 62°$, and for Maui it is at $az = 190°, el = 37°$. Notice the minimum and then increase in the LGS brightness at far northern elevations at the top of the surface plot for Maui.

Figure 4 shows the the results of applying Eq 4 for both the SOR and for Maui. Because the magnetic pole over Maui is so much closer to the horizon, the benefits of pumping with circular polarization are less than for the SOR as indicated by the much larger dark (blue) areas in the sky plots of Fig 4. The brightness of the LGS in the mesosphere at the zenith over the SOR due to the magnetic field is only around 2/3 of the brightness if there were no magnetic field, but there is more than a 50% loss due to the magnetic field at the zenith over Maui. However, as pointed out by Roberts et al [12], the magnetic field is also weaker over Maui, and circular polarization may be disrupted less than for the SOR. Thus, Fig 4 may represent a lower limit for Maui.

6. COMBINING ANNUAL AND DIRECTIONAL MODELS

Combining Eqs 2,3 and 4, gives an expression for predicting the flux of the LGS in the mesosphere over the SOR

$$F_0 = [1.45 - .95 \sin\delta]\ S_0\ t^X w\ [1 - 0.236 \log(1 + t^X w/50.6655)]\ . \qquad 5$$

To predict the flux from the LGS at the top of the telescope Eq 5 has to be adjusted for atmospheric transmission and for the distance to the LGS.

$$F = [1.45 - .95 \sin\delta]\ S_0\ w\ [1 - 0.236 \log(1 + t^X w/50.6655)]\ t^{2X}/X\ . \qquad 6$$

7. TWO FREQUENCY PUMPING

When the D2a line is pumped with one fasor and the D2b line by another, there is an additional increase in brightness over the simple sum of the two fasors. This is because more electrons are made available from the ground state sub-level associated with the D2b transition into the ground state sub-level associated with the D2a transition, thus providing more electrons for optical pumping with circular polarization. When the electrons normally in the D2b sub-level end up getting optically trapped in the D2a transition the guidestar brightness increases because this transition has a higher absorption cross section and back scatter than the D2b transition. While there are theoretical reasons that suggest that simultaneously pumping the two frequencies could result in an approximately 60% (or more) brighter LGS, the difficulty in overlapping the two fasors has restricted our results to lower values. Nevertheless, from several overlap experiments it appears that we can extrapolate to perfectly overlapped spots and predict

$$F = F_A + F_B + (13700/S_0)\ (F_A F_B/4\pi\sigma^2)\ \ , \qquad 7$$

where F_A and F_B are the returns from the individual fasors tuned to D2a and D2b, respectively, and σ is the Gaussian radius of the spot in cm.

We have found that F_B for D2b can be predicted with

$$F_B = F_A/[5/3 + 3.06 \log(1 + t^X w_B/9.48)] \qquad 8$$

where w_B is the B fasor power and F_A here is computed with Eq 6, but with $w = w_B$ and with the magnetic field factor (Eq 4) f set equal to unity in Eq 4 or 6 since D2b is not affected by the magnetic field.

Plugging in Eq 6 for F_A and Eq 8 for F_B into Eq 7, and setting $\sigma = 60$ cm for the apparent size of a spot, Fig 5 shows the return flux of the LGS at the top of the telescope with ($w_A = 45$ W and $w_B = 5$ W) and without ($w_A = 50$ W) two frequency pumping throughout the year for three directions, in the direction of maximum return, and in the opposite azimuth at two elevations.

The enhancement factor for two frequency pumping

$$R = [F_A + F_B + (13700/S_0)\ (F_A F_B/4\pi\sigma^2)]/F^*\ \ , \qquad 9$$

where F^* is Eq 6 if all the power were put into D2a, for the three directions are 1.22, 1.25, and 1.20, respectively, different because of the effect of the magnetic field on F_A. The reason they are so low is that a large spot size of 60 cm was chosen for this example from Section 4.1. A spot size of $\sigma = 45$ cm would increase the enhancements to 1.46, 1.47, and 1.36.

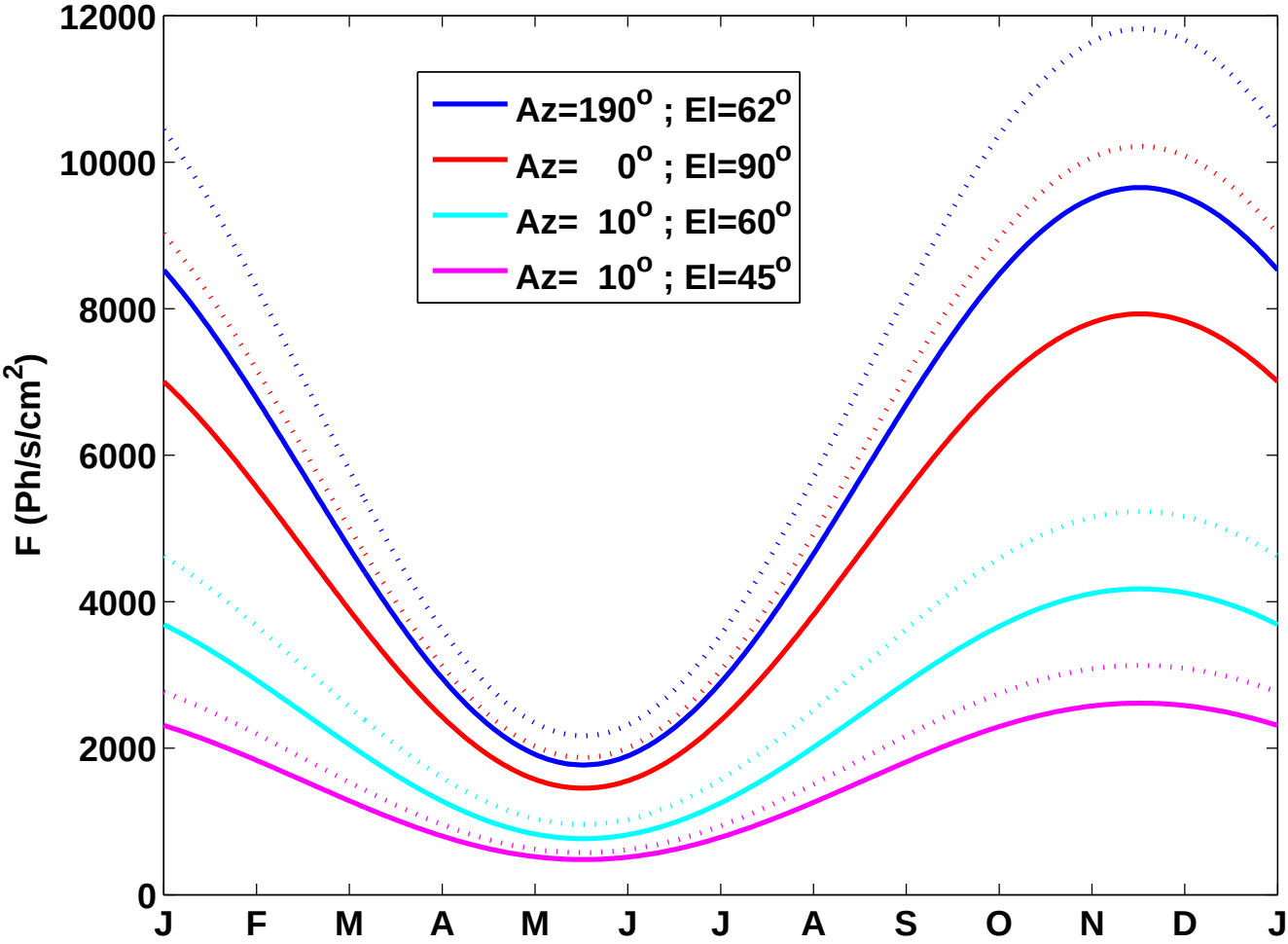

Figure 5. Flux at the top of the telescope for 50 W of power and an atmospheric transmission of 0.83. The solid lines are for the case where all of the 50 W is put into D2a, and the dotted lines are for 45 W into D2a, 5 into D2b, and a spot size of σ = 60 cm. The [Az=190; El=62] curve is for the direction of the magnetic field lines and produces the greatest returns, and [10;60] and [10;45] are the directions of minimum return for the given elevations.

8. SCALING TO MAUI

All of the formulation developed thus far can be applied to the skies over Maui with scaling derived from the extensive measurements of the sodium column density made over both Maui and the SOR by the University of Chicago [12,13]. The mean sodium density throughout the year for Maui is about 85% of the density over the SOR, and the semi-amplitude of its variation is around 50% of the variation over the SOR. Using these to scale the constants, $A = 135$ and $B = 45$ in Eq 2 for Maui. Assuming that the impact of the magnetic field over Maui is the same as over the SOR despite being weaker, Eq 4 can be normalized to the zenith over Maui as $f = 2.10 - 1.37 \sin \delta$, where δ is the angular distance between the fasor pointing and $az = 190°$ and $el = 37°$, the direction of the magnetic field lines over Maui as discussed in Section 5. Otherwise, all of the formulations derived thus far apply to Maui. The impact of the magnetic field over the SOR and over Maui has already been displayed in Fig 4, and Fig 5 for the SOR is repeated for Maui in Fig 6.

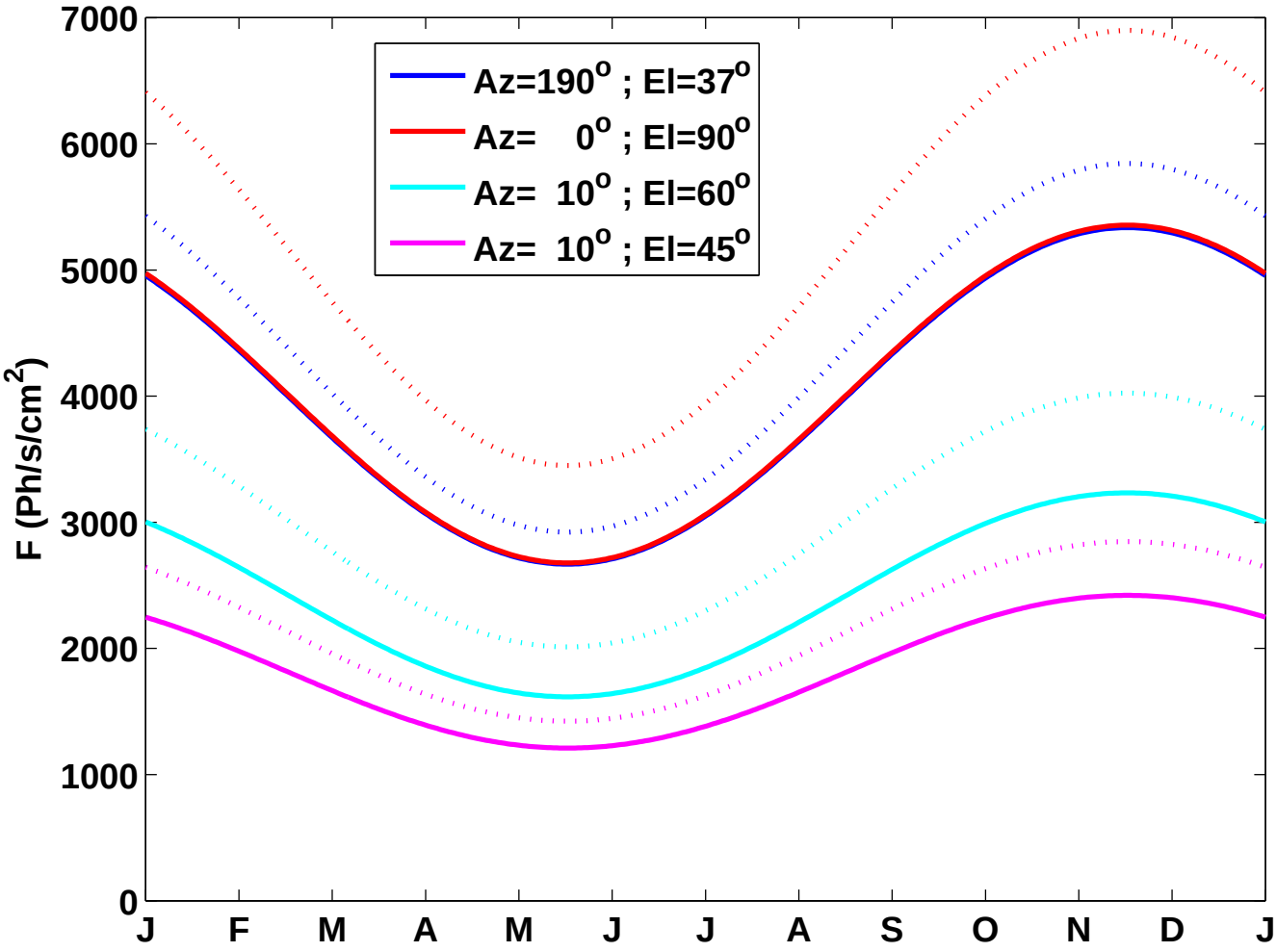

Figure 6. Same as Fig 5, but for Maui. The top solid line is for the direction of the magnetic pole, at an elevation of 37° (instead of the 62° for the SOR), and coincidentally, also corresponds to the zenith for Maui. Notice, however, that two frequency pumping benefits zenith observations much more than when pointing at the magnetic pole.

9. REFERENCES

1. Joshua Bienfang, C. Denman, Brent Grime, P. Hillman, G. Moore, J. Telle, 20 Watt CW All-Solid-State 589-nm Sodium Beacon Excitation Source Based on Doubly Resonant Sum-Frequency Generation in LBO, OSA Trends in Optics and Photonics (TOPS), Advanced Solid-State Photonics, Vol. 83, 111-120, 2003.

2. Denman, C., P. Hillman, G. Moore, J. Telle, J. Drummond, A. Tuffli, 20 W CW 589 nm sodium beacon excitation source for adaptive optical telescope applications, Opt. Mat. **26**, 507-513, 2004.

3. Denman, C., P. Hillman, G. Moore, J. Telle, Realization of a 50-watt facility-class sodium guidestar pump laser, SPIE, **5707**, 46-49, 2005.

4. Denman, C., P. Hillman, G. Moore, J. Telle, J. Preston, J. Drummond, and R. Fugate, 50-W CW Single Frequency 589-nm FASOR, OSA Trends in Optics and Photonics **85**, Advanced Solid-State Photonics, C. A. Denman and I. Sorokina, eds. (Optical Society of America, Washington, DC), 2005.

5. Denman, C., P. Hillman, G. Moore, J. Telle, J. Drummond, S. Novotny, R. Fugate, J. Spinhirne, J. Preston, M. Eickhoff, Recent results using the 50 watt sodium guidestar pump source at the Starfire Optical Range, AMOS Technical Conference 2005.

6. Telle, J., J. Drummond, C. Denman, P. Hillman, G. Moore, S. Novotny, and R. Fugate, Studies of a mesospheric sodium guidestar pumped by continuous-wave sum-frequency mixing of two Nd:YAG laser lines in lithium triborate, SPIE **6215**, 2006.

7. Denman, C., J. Drummond, M. Eickhoff, R. Fugate, P. Hillman, S. Novotny, and J. Telle, Characteristics of sodium guidestars created by the 50-watt FASOR and first closed-loop AO results at the Starfire Optical Range, SPIE **6272**, 62721L-12, 2006.

8. Drummond, J., J. Telle, C. Denman, Paul Hillman, and A. Tuffli, Photometry of a Sodium Laser Guidestar from the Starfire Optical Range, PASP, **116**, 278-289, 2004.

9. Drummond, J., J. Telle, C. Denman, P. Hillman, J. Spinhirne, and J. Christou, Photometry of a Sodium Laser Guidestar from the Starfire Optical Range. II. Compensating the Pump Beam, PASP **116**, 952-964, 2004.

10. Fugate, R., C. Denman, P. Hillman, G. Moore, J. Telle, I. De La Rue, J. Drummond, J. Spinhirne, Progress toward a 50-watt facility-class sodium guidestar pump laser, SPIE **5490**, 1010-1020, 2004.

11. Drummond, J., S. Novotny, C. Denman, P. Hillman, J. Telle, G. Moore, M. Eickhoff, and R. Fugate, Sodium Guidestar Radiometry Results from the SOR's 50 W Fasor, AMOS Technical Conference 2006.

12. Xiong, H., C. Gardner, and A. Liu 2003, Seasonal and nocturnal variations of the mesospheric sodium layer at Starfire Optical Range, New Mexico, *Chinese Journal of Geophysics* **47**, 432-437

13. Roberts, L.C, L.W. Bradford, C.R. Neyman and A.Z. Liu, Measurements of Mesospheric Sodium Abundance above the Hawaiian Islands, *Pub of Astron. Soc. of Pacific*, **119**, 787-792.